EARTH SURFACE PROCESSES AND LANDFORMS
Earth Surf. Process. Landforms (2012)

Published online in Wiley Online Library
(wileyonlinelibrary.com) DOI: 10.1002/esp.3355

Slope failures and erosion rates on a glacierized high-mountain face under climatic changes

Luzia Fischer,[1,2]* Christian Huggel,[2] Andreas Kääb[3] and Wilfried Haeberli[2]
[1] Geological Survey of Norway (NGU), Trondheim, Norway
[2] Department of Geography, University of Zurich, Zurich, Switzerland
[3] Department of Geosciences, University of Oslo, Oslo, Norway

Received 31 May 2011; Revised 2 October 2012; Accepted 10 October 2012

*Correspondence to: Luzia Fischer, Geological Survey of Norway (NGU), Trondheim, Norway. E-mail: luzia.fischer@ngu.no

ESPL
Earth Surface Processes and Landforms

ABSTRACT: In this study, rapid topographic changes and increased erosion rates caused by massive slope failures in a glacierized and permafrost-affected high-mountain face were investigated with respect to the current climatic change. The study was conducted at one of the highest periglacial rock faces in the European Alps, the east face of Monte Rosa, Italy. Pronounced changes in ice cover and repeated rock and ice avalanche events have been documented in this rock wall since around 1990. The performed multi-temporal comparison of high-resolution digital terrain models (DTMs) complemented by detailed analyses of repeat photography represents a unique assessment of topographic changes and slope failures over half a century and reveals a total volume loss in bedrock and steep glaciers in the central part of the face of around 25×10^6 m^3 between 1988 and 2007. The high rock and ice avalanche activity translates into an increase in erosion rates of about one order of magnitude during recent decades.

The study indicates that changes in atmospheric temperatures and connected changes in ice cover can induce slope destabilization in high-mountain faces. Analyses of temperature data show that the start of the intense mass movement activity coincided with increased mean annual temperatures in the region around 1990. However, once triggered, mass movement activity seems to be able to proceed in a self-reinforcing cycle, whereby single mass movement events might be strongly influenced by short-term extreme temperature events. The investigations suggest a strong stability coupling between steep glaciers and underlying bedrock, as most bedrock instabilities are located in areas where surface ice has disappeared recently and the failure zones are frequently spatially correlated and often develop from lower altitudes progressively upwards. Copyright © 2012 John Wiley & Sons, Ltd.

KEYWORDS: periglacial slope instabilities; ice and rock avalanches; topographic changes; erosion rate; climate change

Introduction

Glaciers and permafrost in mountain regions are very sensitive to changes in atmospheric temperature (Haeberli and Beniston, 1998; Harris *et al.*, 2001; IPCC, 2007). As a consequence of climatic variations and changes during the twentieth century, many high-mountain flanks have seen a decrease in glacier cover over the past years and decades (Fischer *et al.*, 2006; Pralong and Funk, 2006) and likely also experienced warming and thaw of permafrost (Harris *et al.*, 2009).

Changes in surface and subsurface ice, especially in combination with unfavourable geological conditions, can reduce the strength of rock and ice and destabilize slopes, thus leading to slope failures such as rock and ice avalanches (Haeberli *et al.*, 1997; Davies *et al.*, 2001; Ballantyne, 2002; Eberhardt *et al.*, 2004; Fischer *et al.*, 2006). Observations of recent large slope failures in mountain regions suggest that such slope stability problems in steep high-mountain faces become increasingly important in view of ongoing climate changes and the hazard potential they present (e.g. Evans and Clague, 1994; Haeberli, 2005; Geertsema *et al.*, 2006; Oppikofer *et al.*, 2008; Allen *et al.*, 2011; Ravanel and Deline, 2011; Fischer *et al.*, 2012). But the evidence is typically ambiguous, and physical cause-and-effect relationships remain speculative. Interacting processes are complex in steep glacierized mountainsides and they have only recently been studied in more detail and in a more comprehensive way, recognizing the fundamental importance of glacier–permafrost linkages for stability of steep ice bodies and rock walls (Alean, 1985; Wegmann *et al.*, 1998; Haeberli, 2005; Pralong and Funk, 2006; Huggel, 2009).

Changes in subsurface ice by permafrost degradation and a rise in the subsurface ice temperature can have – especially in sections of relatively warm permafrost occurrence – a strong impact on the stability of steep rock walls by influencing the geotechnical characteristics of rock discontinuities (Wegmann *et al.*, 1998; Davies *et al.*, 2001; Noetzli *et al.*, 2003). The temperature range from −1 °C to 0 °C is known to be especially critical for slope stability because of the simultaneous occurrence of ice and water in cracks and fissures and a reduction of the shear strength of ice-bonded discontinuities (Davies *et al.*, 2001; Harris *et al.*, 2009; Hasler *et al.*, 2011).

Firn and ice temperatures determined by glacio-climatological factors are known to affect the stability of steep hanging glaciers and probably also underlying bedrock (Alean, 1985; Haeberli *et al.*, 1989; Wagner, 1996). Factors affecting the stability of ice on steep slopes are adhesion of cold and polythermal ice on

bedrock, cohesion with more stable upslope ice, and stabilizing effects from cold ice margins frozen to bedrock (Röthlisberger, 1981; Haeberli *et al.*, 1999a). Climatic changes may introduce complex feedback mechanisms involving changes in surface geometry, ice accumulation rates, firn, en-glacial and sub-glacial temperatures, melt water and stress distribution that may, eventually, reduce the stability of parts of or the entire hanging glacier (Wegmann *et al.*, 1998; Pralong and Funk, 2006).

A loss of surface ice cover on a high-mountain face has an effect on the temperature and stress fields in the underlying bedrock down to great depths (Wegmann *et al.*, 1998; Fischer *et al.*, 2010). If previously ice-covered bedrock becomes exposed to mechanical and thermal erosion, penetration of the freezing front into previously non-frozen material has the potential to intensify rock destruction through ice formation in cracks and fissures (Hallet *et al.*, 1991; Haeberli *et al.*, 1997; Matsuoka *et al.*, 1998; Kneisel, 2003).

Weathering and mass movements in association with freeze–thaw action are fundamental processes modifying periglacial slopes (Matsuoka *et al.*, 1997; Ballantyne, 2002). A number of field studies have been carried out on the distribution and quantity of rockfall as a contributor to erosion and rock wall recession, as well as on erosion rates in glacierized areas (Rapp, 1960; Hallet *et al.*, 1996; Sass, 2005; Rabatel *et al.*, 2008; Krautblatter *et al.*, 2012). They show a large variation of erosion rates in glacierized areas from 0·01 up to 100 mm/yr, depending on study area size, local climate, glacier and bedrock type. However, it is important to recognize that the rate of backweathering (rockwall retreat) and rockfall supply can additionally show significant variations over time (Krautblatter and Dikau, 2007). Thus, strong changes in surface ice and permafrost coverage might cause major re-adjustments in backweathering and sediment transfer within a specific area (Warburton, 2007). However, the influence of ice changes on backweathering in high-mountain rock walls covered by hanging glaciers as well as widespread permafrost occurrence has rarely been investigated.

The Monte Rosa and its glacierized east face in the European Alps is an intriguing example for strong glacial and periglacial changes and slope instabilities. Based on multiple high-resolution digital terrain models (DTMs) recent studies have documented the massive mass loss due to slope failures on this mountainside over the past two decades (Fischer *et al.*, 2011). But important questions regarding climatic and other controls on slope destabilization, failure mechanisms and impacts and dynamics of erosion still remained open. Thus, the objectives of the presented study are to:

- analyse the occurred slope failures and topographic changes based on time series comparisons of high-resolution DTMs and detailed analysis of repeat imagery;
- provide insight into the slope instability progression and process coupling between rock and ice avalanches on the Monte Rosa east face;
- analyse the possible influence of air temperature and radiation on the slope instabilities;
- calculate backweathering rates and debris flux rates in the context of the observed massive topographic changes on the face.

Study Site

The Monte Rosa east face is among the highest rock walls in the European Alps and extends from 2200 m to > 4600 m above sea level (a.s.l.) (45°56′N, 7°53′E, Figure 1). Large sections are covered by steep hanging glaciers and firn fields. Between the last glacial maximum at the end of the Little Ice Age (i.e. around

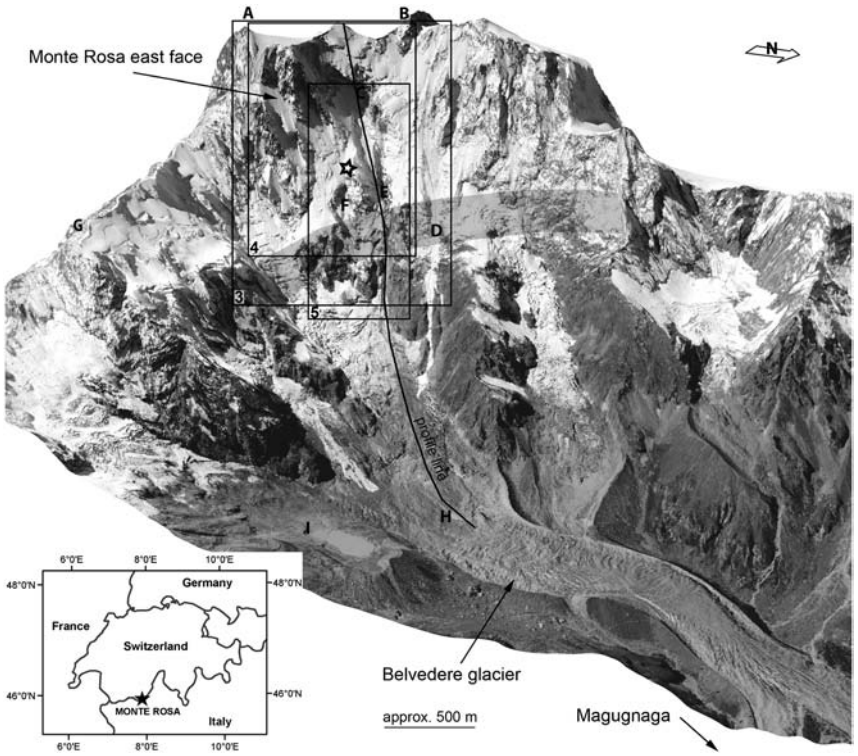

Figure 1. Oblique view on the Monte Rosa east face and the Belvedere Glacier from the northeast. The upper part of the face is assumed to be underlain by continuous permafrost, and the horizontal grey band indicates the approximate lower boundary of permafrost occurrence. A: Signalkuppe, B: Dufourspitze, C: Parete Innominata, D: Marinelli Channel, E: Imseng Channel, F: Zapparoli Channel, G: Punta Tre Amici, H: Lago Effimero, I: Lago delle Loccie. The rectangles show the extent of Figures 3, 4 and 5. The star in the middle is given as an orientation point and indicates the same position as in the photograph comparisons in Figures 3, 4 and 5.

1850) and the 1980s, the hanging glaciers and firn fields on the face have changed only slightly (Fischer *et al.*, 2011). During recent decades, however, the ice cover experienced an accelerated and drastic loss in extent and thickness (Haeberli *et al.*, 2002; Kääb *et al.*, 2004; Fischer *et al.*, 2006, 2011). In Figure 2, the areas with the largest changes are marked, showing a full ice cover still in 1983, and large parts ice-free in 2003. Since about 1990, new slope instabilities have developed in bedrock areas and in hanging glaciers. Frequent small-volume as well as several large-volume rock and ice avalanches and debris flow events have led to significant topographic change.

Bedrock temperature measurements and permafrost modelling have shown that approximately the upper two-thirds of the rock wall are under permafrost conditions. The assumed lower boundary of permafrost is indicated by a grey bar in Figure 1 (Zgraggen, 2005; Fischer *et al.*, 2006). The geological setting is characterized by layers of orthogneiss and paragneiss, with pronounced structural discontinuity sets especially in the paragneiss (Bearth, 1952; Fischer *et al.*, 2006).

The Belvedere Glacier at the foot of the Monte Rosa east face is a humid-temperate, almost entirely debris-covered glacier, which is fed by the steep glaciers and ice avalanches from the face, and extends about 3 km downvalley (Mazza, 2000; Figure 1). The heavy debris cover of the Belvedere Glacier, its thick sediment bed as well as the existence of several huge end and lateral moraines indicate a high long-term debris-turnover in this valley (Mazza, 1998). In the summer 2001, the Belvedere Glacier started a surge-type movement with strongly increased surface velocities and uplifted glacier surface, and the transient supra-glacial lake Lago Effimero developed at the foot of the Monte Rosa in September 2001 and the two following summers (Haeberli *et al.*, 2002; Kääb *et al.*, 2004; Tamburini and Mortara, 2005).

Topographic Changes and Slope Failures

Data and methods

The recent topographic changes in the Monte Rosa east face were documented in detail in Fischer *et al.* (2011) based on a time series of high-resolution DTMs. The DTMs were produced with a final grid resolution of 2 m from high-precision digital aerial photogrammetry for 1956, 1988 and 2001 and from airborne LiDAR (light detection and ranging) taken in 2005 and 2007. More details on data processing, corresponding accuracy and errors can be found in Fischer *et al.* (2011).

Multi-temporal DTM comparisons were performed by calculating the difference between two consecutive DTMs for a quantitative assessment of topographic changes in a certain time interval. Figure 3 shows the difference calculations for four time intervals, whereby all blue areas indicate mass accumulation and the yellow to red areas indicate mass loss. There is no colour shading in areas where apparent change is within ± 5 m. The difference is given in Euclidean distance (e-distance), which is the shortest distance between closest located discrete points on two data sets, corresponding closely to the surface-perpendicular thickness of mass loss and gain. This e-distance is advantageous in such steep terrain over, for instance, vertical differences (z-distance, Fischer *et al.*, 2011).

In this work, we compare these quantitative topographic change analyses with more qualitative analyses of terrestrial photograph sequences in order to obtain a higher temporal resolution and more details about the locations and progression of the slope instabilities (Figures 2, 4 and 5). The photographs are collected from different sources aiming at a high temporal resolution of phases with major changes. Figure 2 gives an overview of the ice cover extent on the mountainside at different stages, Figure 4 depicts the essential changes and mass movement events in the upper part of the slope, whereas Figure 5 focuses on the central part of the face with changing runout paths over time.

Results

In the following, topographics changes and mass movements are chronologically described, pointing out the slope failure progression, shift of active zones and linkage of the different changes/events.

Overall, the DTM comparisons in Fischer *et al.* (2011) revealed a total volume loss of around 25×10^6 m^3 from 1956 until 2007, including both bedrock and glacier ice, whereby the major part of mass loss has occurred since 1988 and in glacier ice. In the photograph comparison in Figure 2, these strong topographic changes become obvious mainly from the striking changes in the ice cover on the face.

1956–1988

Between 1956 and 1988, only minor topographic changes were observed in the ice coverage and none in the bedrock areas (Figure 3a). This result is confirmed by the limited changes evident on photographs from 1911 and 1986 in Figure 4. There are no evidence or reports of mass movement activity in this period.

1988–2001

Significantly different patterns of mass wasting developed between 1988 and 2001. Mass loss of up to 115 m thickness (e-distance) occurred in the steep glaciers and bedrock in the central part of the face, mainly due to gravitational mass movement processes (Figure 3b). Comparison of terrestrial photographs from 1983 and 2003 (Figure 2, upper marking), and 1986 and 2002 (Figure 4), confirm the striking changes in

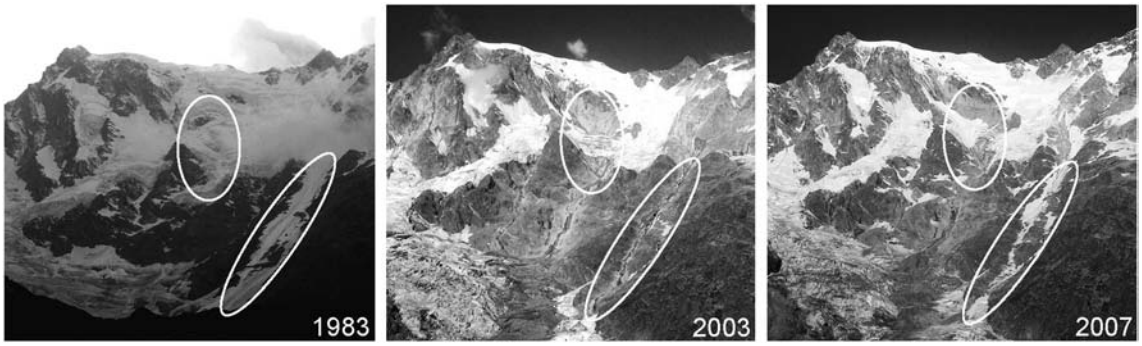

Figure 2. Overview of the strong ice-cover changes in the Monte Rosa east face within two decades. Photographs: 1983 taken by W. Haeberli; 2003 and 2007 taken by L. Fischer.

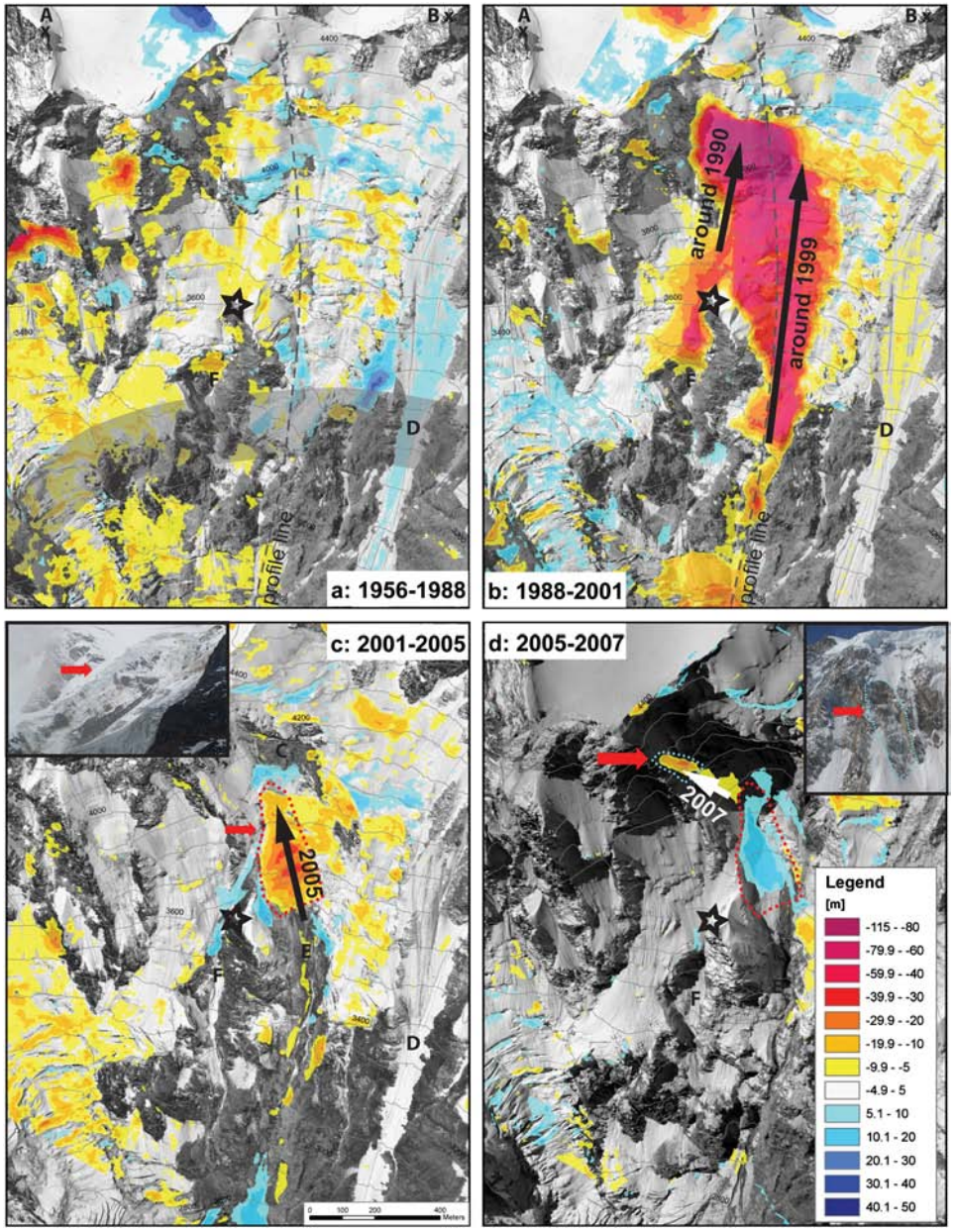

Figure 3. Topographic changes in the central part of the Monte Rosa east face from DTM comparisons in the form of e-difference maps (Euclidean difference); volume loss (yellow to red), volume gain (blue) and no colour shading in areas with apparent changes within ±5 m. The surface differences are plotted on the orthophotos of 1988 (top row), 2001 and 2005; the contour interval is 100 m. Important mass failures and main directions of instability progression are marked with arrows and the location labelling is the same as in Figure 1. The approximate lower limit of the permafrost occurrence is shown in grey in the 1956–1988 graphic and applies to all graphics. The black star in the centre is given as an orientation point and indicates the same position as in Figures 4 and 5.

the area of the Parete Innominata (marked with C), where a complete hanging glacier and large parts of underlying bedrock disappeared within a few years and a steep rock wall became subsequently exposed. The topographic changes in this area (Location 3 in Figures 4, 5 and 6) occurred both, in steep glaciers and bedrock.

Interpretations of terrestrial and aerial photographs and observations by local people reveal that the slope failures started around 1990 in the bedrock at Location 1 (Figures 4 and 5). Subsequently, the hanging glacier above and adjacent bedrock areas failed in a combination of one major and several small-scale rock and ice avalanche events. Interaction between rock avalanche events and glacier retreat caused mass loss further proceeding further upward on the face (progression indicated with an arrow in Figures 3b and 5). The main runout path at this time was the Zapparoli Channel (F) at Location 2.

After this first slope failure period, a phase of reduced mass movement activity followed between 1992 and 1998. Increased gravitational mass movement activities started again around the year 1999, now located in the neighbouring Imseng Channel (E). The lowermost part of the steep glacier disappeared with a remarkable mass loss of up to 60 m thickness between 1999 and 2001 (marked with Location 4 in Figures 4, 5 and 6, and direction of progression is indicated with an arrow in Figure 3b). Mass loss in this area consisted mainly of ice. The mass failures started in the lowest part of the glacier and proceeded progressively upwards in a combination of repeated small-scale events and one major ice avalanche. This intensive ice avalanche activity, combined with rockfall and debris flow activity from newly ice-free areas, caused along the runout channel up to 40 m erosion of the glacier ice, what is also visible in the lowest part of the profile (Figure 6).

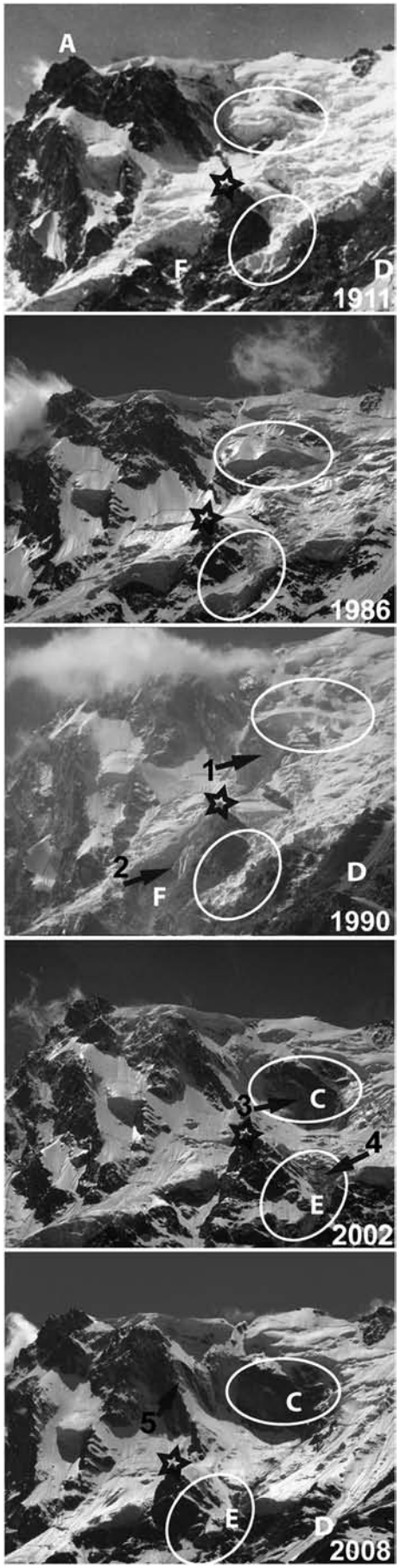

Figure 4. Detailed analyses of topographic changes from visual photograph analyses (upper part of the face). The zones of major changes are marked and the location numbering is the same as in Figures 1 and 3. Photographs: around 1911 taken by the brothers Wehrli, 1986 and 1990 by H. Röthlisberger, 2002 by W. Haeberli, 2008 by L. Fischer.

2001–2005

After ongoing rockfall and debris flow activity over several years from the newly ice-free area in the Imseng Channel (E) and mainly from right below the current hanging glacier front, the slope failure activity in this area culminated in August 2005 in a single ice avalanche event with a maximum detachment thickness of 40 m, resulting in a total volume of around $1{\cdot}2 \times 10^6$ m^3 (Figures 3c and 5). The volume of the 2005 ice avalanche is among the largest documented in the European Alps over the past 100 years (cf. http://www.glacierhazards.ch/). The increasing rockfall and debris flow activity just below the glacier front seemed to have destabilized the entire glacier. An additional destabilizing factor might also be the accumulation of rockfall talus on the hanging glacier from the unstable Parete Innominata rock wall (C) above.

2005–2007

From 2005 to 2007 considerable ice volume gain with up to 20 m thickness took place in the area of the former detachment zone of the 2005 ice avalanche in the Imseng Channel (Figure 3d and Figure 4). In April 2007 a rock avalanche detached from the uppermost part of the face where continuous permafrost occurrence was expected. This detachment zone of the April 2007 rock avalanche is evident (marked with an arrow in Figure 3d) and the difference between the 2005 and 2007 LiDAR DTMs shows that the detached rock mass was 15–30 m thick (e-distance), resulting in a volume of $0{\cdot}2 \times 10^6$ m^3. The detachment zone is directly located above the area where the mass movement activity started in 1990 and where strong mass loss occurred since then, mainly in bedrock but also in ice.

Slope failure progression

The DTM comparisons and imagery analyses revealed that the sequence of ice-cover changes and slope failures is strongly spatially correlated, often moving from lower altitudes progressively upwards. The slope failures started in 1990 and continued in several phases with increased activity, located in different zones on the face. Such detailed slope failure progression analyses cannot be done based solely on the DTM comparisons but need a higher temporal resolution and imagery data to be able to distinguish between rock and ice. From such detailed imagery analyses, field observations and information from locals it becomes obvious that the instabilities often occur first in steep glaciers and subsequently in underlying bedrock. Thus, most bedrock instabilities are located in areas where surface ice has disappeared recently. But the reversed process sequence was also observed, as around 1990 and for the 2005 ice avalanche, where orthophoto and oblique image analysis show that the instability and slope failure process started in the underlying bedrock and caused subsequent instabilities in the ice.

Large-volume failures from the Monte Rosa east face during the observational period are often preceded by frequent small-volume events, such as observed for all large failures in the periods with permanent high activity around 1990 and 2000. These ice avalanches and combined rock/ice avalanches were also followed by further small-volume events, which shows that the slope equilibrium was not yet recovered and the self-reinforcement of slope failures kept going on. However, the major rock avalanche event in 2007 seems to have occurred without remarkable pre- or post-events. After 2005, the overall situation seemed to stabilize, and less small-volume failures were observed.

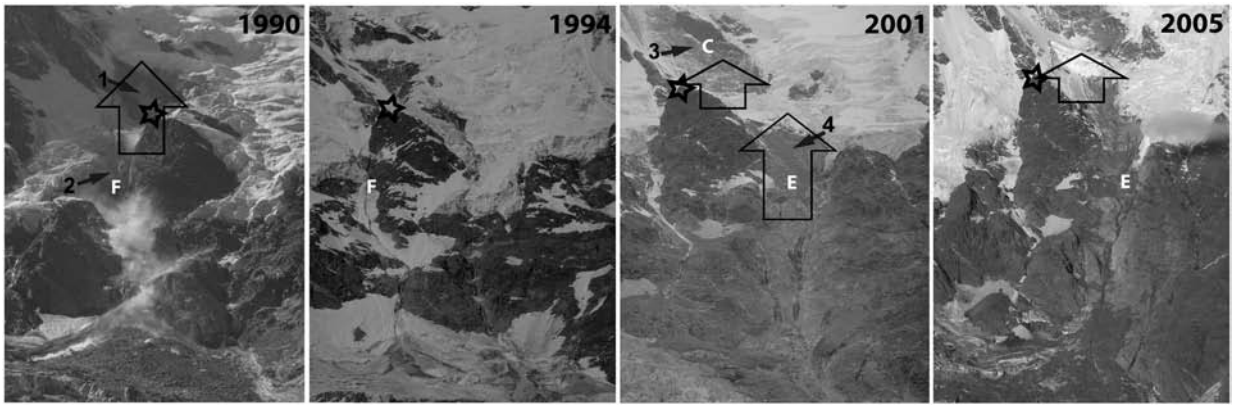

Figure 5. Detailed photographs of the middle part of the face. The areas with high activity and progression directions of the slope instabilities are marked with arrows, and the location numbering is the same as in Figures 1 and 3. Photographs: 1990 and 1994 taken by H. Röthlisberger, 2001 by W. Haeberli, 2005 by L. Fischer. The black star is given as an orientation point and indicates the same position as in Figures 3 and 4.

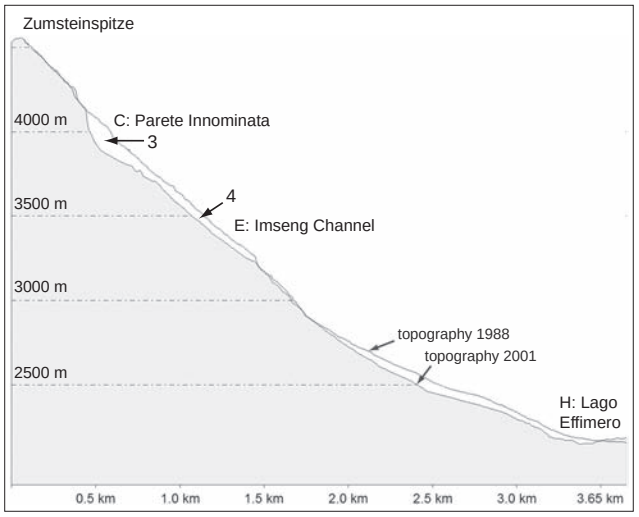

Figure 6. The topographic profiles in the central part of the Monte Rosa east face for the years 1988 and 2001, show massive surface changes over large parts of the face. The zones of major changes are marked and the location numbering is the same as in Figures 1 and 3. The location of the profile is indicated in Figures 1 and 3.

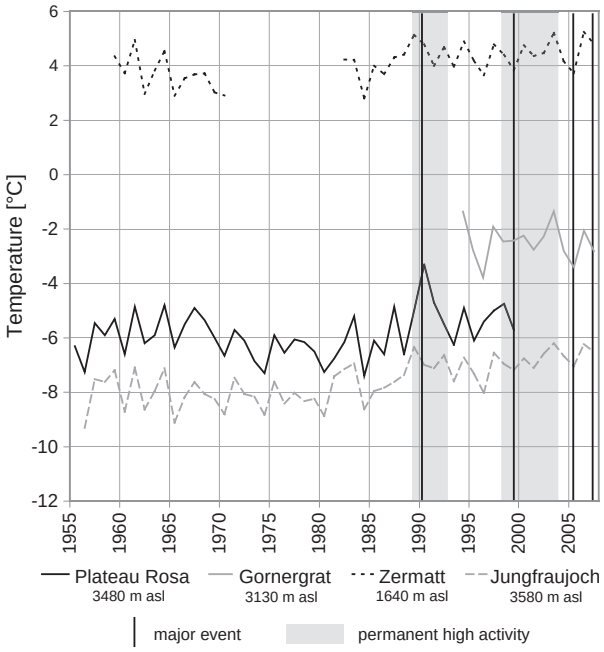

Figure 7. Mean annual air temperature (MAAT) at different sites located close to or at similar altitude as the Monte Rosa east face from 1955 to 2007. The vertical black lines mark major rock and ice avalanche events in the Monte Rosa east face (volumes larger than $0{\cdot}2 \times 10^3$ m^3), the grey areas indicate periods with permanent high mass movement activity.

Climate and Slope Destabilization

Data and methods

Meteorological data were used in the analysis of the potential effects of recent atmospheric warming on the development of slope instabilities and observed slope failures on the Monte Rosa east face. Figure 7 shows the mean annual air temperatures (MAATs) at different sites located close to or at a similar altitude as the Monte Rosa east face. Plateau Rosa is located at 3480 m a.s.l. and at a distance of about 12 km. Gornergrat is a further high-altitude station (3130 m a.s.l.) while Zermatt represents a valley station (1640 m a.s.l.), at 10 and 15 km distance of Monte Rosa, respectively. The Jungfraujoch meteorological station is located in the Bernese Alps about 65 km north of Monte Rosa at 3580 m a.s.l. As can be inferred from Figure 7, the MAAT of the regional high-elevation stations are highly correlated (correlation coefficient of 0·98 for the long-term record of Gornergrat and Jungfraujoch).

In addition, Figure 7 shows periods with enhanced mass movement activity to enable comparison of the timing of slope failure events with the temperature data. Vertical black lines mark major rock and ice avalanche events (volume $0{\cdot}2 \times 10^3$ m^3), the grey shaded areas indicate periods with permanent high activity of small-scale events.

Air temperature and global radiation data of up to 30 days before the rock slope failures in April 2007 and September 2010 were collected (Figure 8) to investigate a possible influence of short-term temperature extremes on slope failure triggering (Huggel *et al.*, 2010). Maximum air temperatures were extrapolated from the closest high-elevation meteorological station, Gornergrat at 3130 m a.s.l. at 10 km distance, using a lapse rate of 0·65 °C/100 m. The average temperatures over the same time period for the time period of operation of the station (1994–2007) are provided for comparison.

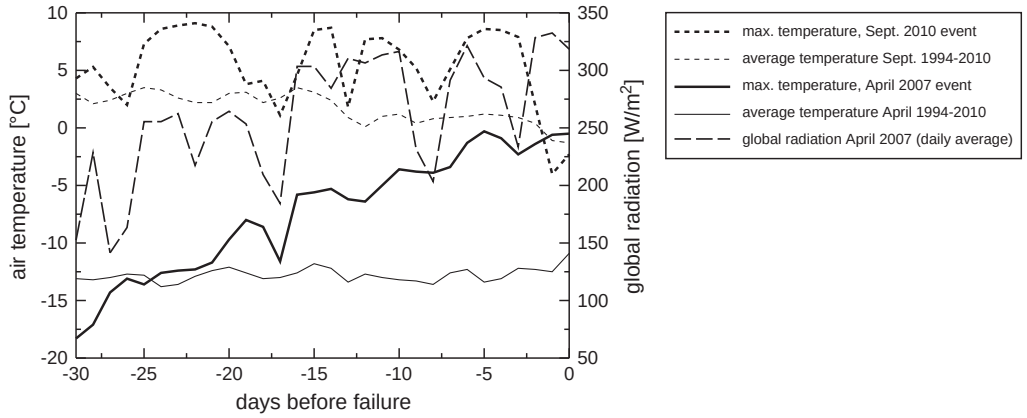

Figure 8. Air temperature and global radiation up to 30 days before the rock slope failures in April 2007 and September 2010. Maximum air temperatures are extrapolated from the closest high-elevation meteorological station, Gornergrat at 3130 m a.s.l. at 10 km distance, using a lapse rate of 0·65 °C/100 m. For comparison the average temperatures over the same time period for the time period of operation of the station (1994–2007) are provided. Global radiation data for April 2007 is from Jungfraujoch station, located at 3580 m a.s.l. in the Central Alps.

Results

Overall, linear regression shows that the MAATs rose by about 0·5 °C to 1·5 °C from 1955 to 2007, or 0·1–0·3 °C/decade, depending on the station. A particularly important temperature increase was observed from about 1989 to 1991 at Plateau Rosa (Figure 7), the station that likely best represents conditions at Monte Rosa east face. The coincidence of the start of intense terrain changes with increased mean annual temperatures around 1990 suggests a strong influence of the thermal conditions on the stability of hanging glaciers and steep bedrock. A comparison of the slope failure zones with the modelled permafrost distribution (Figure 3) shows that all detachment zones are located in permafrost areas. The firn and glacier ice in these areas are assumed to be cold to polythermal. Changes in permafrost temperatures or the polythermal regions of hanging glaciers due to increased air temperatures may locally influence temperatures in the bedrock down to several decametres depth (Wegmann *et al.*, 1998; Huggel, 2009) and increase the possibility of percolating water in fractures in warm sections. This degradation by advection can lead to the quick and deep development of thaw corridors along fractures in permafrost, and potentially destabilize much larger volumes of rock than conduction would (Gruber and Haeberli, 2007). The small-volume rockfall events, which occurred in the area of the Imseng Channel, the Parete Innominata and elsewhere on the face may relate to enhanced thawing within the near-surface active layer of the permafrost or enhanced frost weathering after deglaciation.

No significant changes are detectable in the mean annual temperatures for the period of renewed strong slope failure activity starting around 1999. However, on top of decade and century-scale warming resulting in glacier shrinkage and thawing and warming of permafrost, shorter periods of high temperatures can decrease the stability of high-mountain rock slopes and steep glaciers. In a recent study, Huggel *et al.* (2010) found a consistent pattern of very warm temperatures up to 30 days prior to several major slope failures in glacial and periglacial areas around the world. Here we analyse two important rock slope failures at Monte Rosa, the April 2007 rock avalanche (~200 000 m^3) that detached from around 4000 m a.s.l. below Signalkuppe, and the September 2010 rock slope failure from Punta Tre Amici (~100 000 m^3).

The occurrence of a large rock avalanche from high elevation as early as April is unusual. In fact, an extraordinary spring heat wave occurred in April 2007 over central Europe and the Alps. At the high-elevation station of Jungfraujoch (3580 m a.s.l.) in the central Swiss Alps the April 2007 average temperatures were 5 °C warmer than the average of the preceding 50 years (Huggel *et al.*, 2010). As shown in Figure 8, maximum temperatures gradually increased in April 2007 and reached values close to melting five days before failure. The record of global radiation from Jungfraujoch is evidence of the particularly high radiation during this time, especially two weeks before failure with many days 300 W/m^2, while the long-term (1981–2011) average for April is 226 W/m^2. It is likely that such high radiation in combination with air temperatures close to 0 °C implied melting even at the high elevation of the failure zone of the 2007 rock avalanche. Infiltration of liquid water from melting of snow, firn and ice into the joint system of bedrock could have reduced the shear strength of the slope-parallel layered rock mass. Furthermore, warm conditions in fall 2006 could have played a role by warming the subsurface bedrock to a few metres depth.

Before the 2010 rock slope failure from Punta Tre Amici, repeated periods of high maximum temperatures of up to 8 °C occurred during the 30 days preceding failure, which likely generated significant amounts of meltwater. Just two days before failure, temperatures had dropped to below freezing. Such sudden temperature drops just before slope failures have been observed for a number of other similar events and can cause 'lock-off' conditions (Fischer *et al.*, 2010; Huggel *et al.*, 2010): surface refreezing of liquid water after infiltration can imply a sudden change of pressure conditions in the subsurface bedrock and possibly trigger a slope failure.

Erosion Rates Relating to the Topographic Changes

Methods and results

The massive moraines around the glaciers in the valley and the elevated sediment bed of the Belvedere Glacier are evidence of significant long-term debris production primarily resulting from erosion of the large Monte Rosa east face. Furthermore, photographs from 1895 document that the Belvedere Glacier was totally debris-covered already at that time. This raises

important questions on erosion rates on the Monte Rosa east face. Strong topographic changes due to recent slope failures, which have no historical precedence in that area, suggest an increase in erosion for recent decades.

We applied two approaches to estimate both the sediment flux and backweathering rates over the twentieth century and additionally the ones over the last two decades. An assessment of the more long-term debris flux rate (long-term referring here to the century timescale) was performed based on a bottom-up estimate using glacier debris cover flux rates. It is based on the back-calculation of the debris deposits on the valley glacier Belvedere as related to the contributing rock wall area (Fischer, 2004). The second approach, the so-called top-down approach, focuses on more recent debris flux rates since the increased mass movement activity started towards the end of the twentieth century, and was calculated directly from mass loss deduced from the DTM comparisons of the Monte Rosa east face. The assessment of sediment flux and erosion rates is not intended to be highly accurate but lays more emphasis on obtaining the order of magnitude and an estimate about the impact of increased slope failure activity.

Required parameters for the bottom-up approach were the debris cover thickness on the valley glacier, the glacier flow velocity, the glacier width, and the contributing area on the face. The direct catchment area of the Belvedere Glacier is 9.5 km^2, of which around 4.5 km^2 is bedrock area (a) (Figure 9). The glacier width (w) is 500 m on average. The glacier surface velocity (v) was estimated based on photogrammetric analyses by Kääb (2005), and was on average 30–40 m/yr between 1995 and 1999 (i.e. before the surge-type movements starting in 2001). These surface velocities should be a reasonable average for the twentieth century. The debris cover thickness (h) varied over the glacier. It was measured at different locations by means of direct field surveying. The orographic right glacier tongue showed locally a debris cover thickness up to 1 m, but was on average around 50 cm over larger areas. The left glacier tongue had a debris cover with average thickness of 5 to 30 cm. Our measurements match the extensive debris thickness measurements by Diolaiuti *et al.* (2003) well. They report around 5 cm in the uppermost part of the valley glacier, and 20–30 cm on the glacier tongues, with peak levels of 80 cm on depressions. Ranzi *et al.* (2004) report with around 30 cm debris thickness similar values.

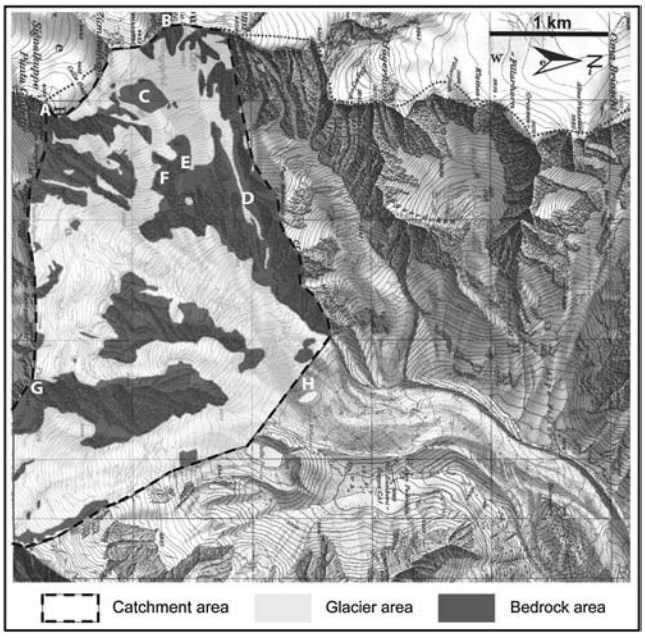

Figure 9. Catchment area that is considered as direct contributing area of the Belvedere Glacier for the erosion rate calculations. The letters are given for orientation and correspond to the labelling in Figure 1. Topographic map reproduced by permission of swisstopo (BA12041).

The sediment flux (f) is then given by:

$$f = (v \times w \times h) \tag{1}$$

and the erosion rate (r) per year is then given by:

$$r = f/a \tag{2}$$

To give consideration to the high variability and uncertainty of all parameters, but mainly the debris thickness, we made calculations for two scenarios:

for $h = 0{\cdot}2$ is $f = 4000$ m^3/yr and $r = 0{\cdot}9$mm/yr

for $h = 0{\cdot}4$ is $f = 8000$ m^3/yr and $r = 1{\cdot}8$mm/yr

The deposits from recent large slope failures in 2005 and 2007 were not included in the calculations of the sediment flux and erosion rate on a century scale as our aim in applying this method was to obtain the sediment flux of the twentieth century before the increased activity. The debris within and below the glacier was also not considered in our calculations, as there was no possibility to assess the amount. Therefore, the value of 0·9 to 1·8 mm/yr can be said to represent the lower boundary of possible erosion rate in this face.

For the top-down approach, the total volume loss within the last 20 years was calculated from the 1988 and 2007 DTMs by a difference calculation in ArcGIS. The calculated elevation difference between the two DTMs was integrated over the area with changes, adding up to a total volume of 25×10^6 m^3 of mass loss. Detailed imagery analyses revealed that the majority of this volume was ice, but no quantitative assessment of the proportion could be performed based on the available data. We roughly estimate that only about 20–30% was bedrock. By dividing the eroded bedrock volume of approximately 5×10^6 m^3 by the time period of 20 years, we obtained a value of 250 000 m^3/yr for the sediment flux. By projecting this material onto the previously considered contributing area (Equation 2), we arrived at an erosion rate of around 50 mm/yr.

Comparison of the sediment fluxes

Although these two approaches for erosion rate assessment actually represent more point estimates for one single location, they are in good agreement with more regional estimates (Hallet *et al.*, 1996) and other studies from the Alps. Barsch (1977; cf. also Haeberli *et al.*, 1999b) calculated values of 1 to 2·5 mm/yr for the Holocene weathering rates for different rocks in the Swiss Alps. Rates of 0·05 to 3 mm/yr were calculated by Francou (1988, in Ballantyne and Harris, 1994) for today's weathering of various rocks in the French Alps. Hoffmann and Schrott (2002) did back-calculations of a weathering rate on the basis of seismic refraction measurements of the thickness of talus slopes. They obtained a range from 0·1 to 1 mm/yr with a mean of 0·5 mm/yr for the post-glacial period.

Results from the bottom-up and top-down approach for the Monte Rosa east face reveal that recent short-term debris flux rates have increased by about two orders of magnitude and the erosion rates by one order of magnitude as compared to twentieth century averages. Thus, the recent massive slope failures on Monte Rosa provoke a highly increased sediment

flux that is comparable to the high rates in the tectonically active ranges of southeast Alaska (Hallet *et al.*, 1996).

Discussion

The observed development of increased mass movement processes since about 1990 indicates strong changes in stability on the face. Small-scale rockfall and ice avalanche events in glacierized high-mountain rock walls are common due to steepness, gravity and weathering. Small ice avalanches from the front often correspond to the natural ablation of steep hanging glaciers. Furthermore, fast changes in surface geometry and disappearance/recovering of hanging glaciers are known to be comparatively independent of climatic conditions, for other high-mountain faces as well (Post and Lachapelle, 1971; Pralong and Funk, 2006). However, the numerous major rock and ice avalanche events since about 1990 with a total volume of around 25×10^6 m^3 have no documented historical precedence of similar magnitude in the European Alps. Furthermore, the assessment of erosion and debris flux rates shows that these slope failures have caused a recent debris flux rate which is roughly two orders of magnitude higher and erosion rates one order of magnitude larger than the century-long average rates. A more systematic comparison to other regions worldwide is difficult because there is no similarly detailed study of mass changes in a large alpine face as presented here. Nevertheless, the observation of several recent high-magnitude slope failures from glacial and periglacial areas around the world with single events in the order of several tens of millions of cubic metres (e.g. Lipovsky *et al.*, 2008; Huggel *et al.*, 2010) suggests that mass movement processes of similar magnitude and time periods are not unique under current warming conditions.

With reference to impacts from climatic change, this study shows that perturbations of the delicate slope equilibrium in glacierized rock walls, such as those induced by a rise in air temperature, can trigger persistent and self-reinforcing slope destabilization accompanied by important slope failures. The coincidence of the start of intense terrain changes with increased mean annual temperatures around 1990 suggests a strong influence of air temperatures and related thermal penetration in surface and subsurface bedrock and glacier ice. Enhanced percolation of liquid water from the melting of snow, firn and ice has likely reduced the strength of steep glacier ice and rock, e.g. by infiltration into cleft systems. Furthermore, changes in temperature, precipitation, or solar radiation can imply changes in snow and ice accumulation and ablation patterns to which small and steep glaciers are rapidly responding (cf. Figure 4, rapid ice accumulation between 2005 and 2007). Quantitative data and field observations suggest that such climatically related changes in glacier ice and bedrock may induce small-volume as well as large-volume slope failures. The observed slope failures are mostly spatially connected, starting in one area and often proceeding with a slope failure chain reaction from lower to higher elevation. The chain reaction documented here can at some point develop independent of further climatic changes, and be driven by mechanical and thermal self-reinforcement processes until the topography again reaches a state of meta-stability.

A distinct pattern of temporal and spatial distribution of the slope failures was observed. The major rock and ice avalanches typically occurred in periods where mass movement activity was generally high (Figure 7). This suggests that large slope instabilities are often preceded by high-frequency but low-volume failures, and that the affected slope becomes not stable right after a major event, as documented at several other sites as well (e.g. Lipovsky *et al.*, 2008). However, some large-volume events occurred without direct precursory activity (e.g. the rock avalanche event in April 2007). For the 2007 rock avalanche event, the response of steep bedrock areas to glacier retreat, at the same time, is strongly conditioned by the geological setting, in particular by the geometrical and geotechnical characteristics of discontinuities. This rock avalanche was obviously a consequence, with a delay of some years, of the combination of enormous mass loss of over 15×10^6 m^3 ice and bedrock directly adjacent to this area, inducing strong changes in the internal stress field, and a surface-parallel setting of the rock discontinuities, making the slope prone to failure.

Our study shows that changes in surface geometry and surface cover of partially glaciated rock walls can be rapid, and vary considerably in process, magnitude and timing over a large mountainside. External factors such as climatic changes may trigger the onset of significant changes in surface ice properties and mass movement activity. However, some of the resulting topographic changes can lead to self-reinforcing and irreversible process chains with strongly increasing mass movement activity, potentially resulting in large-volume rock and ice avalanches. The high erosion rates of the face and enormous sediment volumes in the valley indicate that this mountainside experienced high mass turnover already in recent centuries. However, the current situation is considered to be unprecedented, and slope stability equilibrium not yet reached.

Conclusions

The results of the multi-temporal DTM comparison and imagery analysis in this study represent a unique documentation and quantitative assessments of topographic changes in ice and bedrock in a large glacierized alpine face over half a century. A dataset of exceptional temporal and spatial resolution, and the application of different methodological approaches allow for insights into recent changes of slope failure activity and erosion rates.

The following conclusions are drawn for this study:

- the total volume loss in bedrock and steep glaciers in the central part of the face is around 25×10^6 m^3 from 1988 to 2007;
- the investigations suggest a strong process and stability coupling between steep glaciers and underlying bedrock;
- most bedrock instabilities are located in areas where surface ice has disappeared recently;
- failure zones are spatially correlated and often proceed from lower altitudes progressively upwards;
- the start of intense mass movement activity coincides with strongly increased mean annual temperatures around 1990;
- the two rock avalanches in 2007 and 2010 investigated in more detail were both preceded by a series of extremely, unseasonably warm days;
- once started, topographic and ice-cover changes can lead to a self-reinforcing mass movement cycle with iterative small and large-volume slope failures;
- the recent mass failures have increased the erosion rates on the face by one order of magnitude.

Permafrost bedrock and steep glaciers in cold mountain regions will continue to be affected by climatic changes, and consequently, comparable glacial changes and slope instabilities might also develop on other periglacial mountainsides.

Acknowledgements—The authors would like to thank Henri Eisenbeiss, Hans Röthlisberger, Gianni Mortara, Andrea Tamburini, Marta Chiarle, Paolo Semino, the Rifugio Zamboni crew, and the Dipartimento di

Protezione Civile, Regione Piemonte, Regional Valle d'Aosta. Special thanks are due to two anonymous referees for constructive reviews that helped improve this contribution. Provision of temperature data by MeteoSwiss is acknowledged. The authors acknowledge support and funding from the Swiss National Science Foundation (Project no. 200021–111967).

References

Alean JC. 1985. Ice avalanches: some empirical information on their formation and reach. *Journal of Glaciology* **31**: 324–333.

Allen SK, Cox SC, Owens IF. 2011. Rock avalanches and other landslides in the central Southern Alps of New Zealand: a regional study considering possible climate change impacts. *Landslides* **8**: 33–48. DOI. 10.1007/s10346-010-0222-z

Barsch D. 1977. Eine Abschätzung von Schuttproduktion und Schutttransport im Bereich aktiver Blockgletscher der Schweizer Alpen. *Zeitschrift für Geomorphologie N.F.* **28**: 148–160.

Ballantyne CK. 2002. Paraglacial geomorphology. *Quarternary Sciences Review* **21**: 1935–2017.

Ballantyne CK, Harris C. 1994. *The Periglaciation of Great Britain*. Cambridge University Press: Cambridge; 330.

Bearth P. 1952. Geologie und Petrographie des Monte Rosa. *Beiträge zur Geologischen Karte der Schweiz*. Schweizerische Geologische Kommission: Bern.

Davies MCR, Hamza O, Harris C. 2001. The effect of rise in mean annual temperature on the stability of rock slopes containing ice-filled discontinuities. *Permafrost and Periglacial Processes* **12**(1): 137–144.

Diolaiuti G, D'Agata C, Smiraglia C. 2003. Belvedere glacier, Monte Rosa, Italian Alps: tongue thickness and volume variations in the second half of the 20th century. *Arctic, Antarctic, and Alpine Research* **35**(2): 255–263.

Eberhardt E, Stead D, Coggan JS. 2004. Numerical analysis of initiation and progressive failure in natural rock slopes – the 1991 Randa rockslide. *International Journal of Rock Mechanics & Mining Sciences* **41**: 69–87.

Evans SG, Clague JJ. 1994. Recent climatic change and catastrophic geomorphic processes in mountain environments. *Geomorphology* **10**: 107–128.

Fischer L. 2004. Monte Rosa Ostwand – Geologie, Vergletscherung, Permafrost und Sturzereignisse in einer hochalpinen Steilwand. Diploma Thesis, Department of Earth Sciences, ETH Zurich.

Fischer L, Amann F, Moore JR, Huggel C. 2010. Assessment of periglacial slope stability for the 1988 Tschierva rock avalanche (Piz Morteratsch, Switzerland). *Engingeering Geology* **116**(1–2): 32–43.

Fischer L, Eisenbeiss H, Kääb A, Huggel C, Haeberli W. 2011. Monitoring topographic changes in a periglacial high-mountain face using high-resolution DTMs, Monte Rosa east face, Italian Alps. *Permafrost and Periglacial Processes* **22**: 140–152. DOI. 10.1002/ppp.717

Fischer L, Kääb A, Huggel C, Noetzli J. 2006. Geology, glacier retreat and permafrost degradation as controlling factors of slope instabilities in a high-mountain rock wall: the Monte Rosa east face. *Natural Hazards and Earth System Sciences* **6**: 761–772. DOI. 10.5194/nhess-6-761-2006

Fischer L, Purves RS, Huggel C, Noetzli J, Haeberli W. 2012. On the influence of topographic, geological and cryospheric factors on rock avalanches and rockfalls in high-mountain areas. *Natural Hazards and Earth System Sciences* **12**: 241–254.

Francou B. 1988. L'Eboulisation en haute montagne. Andes et Alpes. Editec, Caen, 2 tomes. 696 pp. Glacier hazards. http://www.glacierhazards.ch [23 April 2012]

Geertsema M, Clague JJ, Schwab JW, Evans SG. 2006. An overview of recent large catastrophic landslides in northern British Columbia, Canada. *Engineering Geology* **83**: 120–143.

Gruber S, Haeberli W. 2007. Permafrost in steep bedrock slopes and its temperature-related destabilization following climate change. *Journal of Geophysical Research* **112**: F02S18. DOI. 10.1029/2006JF000547

Haeberli W. 2005. Investigating glacier–permafrost relationships in high-mountain areas: historical background, selected examples and research needs. In *Cryospheric Systems: Glaciers and Permafrost*, Harris C, Murton JB (eds). The Geological Society of London, Special Publication 242. The Geological Society: London; 29–37.

Haeberli W, Alean J, Müller P, Funk M. 1989. Assessing risks from glacier hazards in high mountain regions: some experiences in the Swiss Alps. *Annals of Glaciology* **13**: 96–102.

Haeberli W, Beniston M. 1998. Climate change and its impacts on glaciers and permafrost in the Alps. *Ambio* **27**(4): 258–265.

Haeberli W, Kääb A, Hoelzle M, Bösch H, Funk M, Vonder Mühll D, Keller F. 1999a. *Eisschwund und Naturkatastrophen im Hochgebirge*. vdf Hochschulverlag an der ETH Zürich: Zürich; 190.

Haeberli W, Kääb A, Paul F, Chiarle M, Mortara G, Mazza A, Deline P, Richardson S. 2002. A surge-type movement at Ghiacciaio del Belvedere and a developing slope instability in the east face of Monte Rosa, Macugnaga, Italian Alps. *Norwegian Journal of Geography* **56**: 104–111.

Haeberli W, Kääb A, Wagner S, Vonder Mühll D, Geissler P, Haas JN, Glatzel-Mattheier H, Wagenbach D. 1999b. Pollen analysis and ^{14}C age of moss remains in a permafrost core recovered from the active rock glacier Murtèl-Corvatsch, Swiss Alps: geomorphological and glaciological implications. *Journal of Glaciology* **45/149**: 1–8.

Haeberli W, Wegmann M, Vonder MD. 1997. Slope stability problems related to glacier shrinkage and permafrost degradation in the Alps. *Eclogae Geologicae Helveticae* **90**: 407–414.

Hallet B, Hunter L, Bogen J. 1996. Rates of erosion and sediment evacuation by glaciers: a review of field data and their implications. *Global and Planetary Changes* **12**(1–4): 213–235.

Hallet B, Walder JS, Stubbs CW. 1991. Weathering by segregation ice growth in microcracks at sustained subzero temperatures: verification from experimental study using acoustic emissions. *Permafrost and Periglacial Processes* **2/4**: 283–300.

Harris C, Arenson LU, Christiansen HH, Etzelmüller B, Frauenfelder R, Gruber S, Haeberli W, Hauck C, Hölzle M, Humlum O, Isaksen K, Kääb A, Kern-Lütschg MA, Lehning M, Matsuoka N, Murton JB, Nötzli J, Phillips M, Ross N, Seppälä M, Springman SM, Vonder MD. 2009. Permafrost and climate in Europe: monitoring and modelling thermal, geomorphological and geotechnical responses. *Earth-Science Reviews* **92**(3–4): 117–171.

Harris C, Davies M, Etzelmüller B. 2001. The assessment of potential geotechnical hazards associated with mountain permafrost in a warming global climate. *Permafrost and Periglacial Processes* **12**: 145–156.

Hasler A, Gruber S, Font M, Dubois A. 2011. Advective heat transport in frozen rock clefts: conceptual model, laboratory experiments and numerical simulation. *Permafrost and Periglacial Processe* **22**(4): 378–389. DOI. 10.1002/ppp.737

Hoffmann T, Schrott L. 2002. Modelling sediment thickness and rockwall retreat in an Alpine Valley using 2D-seismic refraction (Reintal, Bavarian Alps). *Zeitschrift für Geomorphologie N.F.* **127**: 153–173.

Huggel C. 2009. Recent extreme slope failures in glacial environments: effects of thermal perturbation. *Quaternary Science Reviews* **28**: 1119–1130. DOI. 10.1016/j.quascirev.2008.06.007

Huggel C, Salzmann N, Allen SK, Caplan-Auerbach J, Fischer L, Haeberli W, Larsen C, Schneider D, Wessels R. 2010. Recent and future warm extreme events and high-mountain slope stability. *Philosophical Transactions of the Royal Society A* **368**: 2435–2459.

Intergovernmental Panel on Climate Change (IPCC). 2007. Climate change 2007: the physical science basis. In *Contribution of Working Group 1 to the Fourth Assessment Report of the Intergovernmental Panel on Climate Change*, Solomon S, Qin D, Manning M, Chen Z, Marquis MC, Averyt K, Tignor M, Miller HL (eds). IPCC: Cambridge.

Kääb A. 2005. *Mountain Glaciers and Permafrost Creep. Methodical Research Perspectives from Earth Observation and Geoinformatics Technologies*. Habilitationsschrift, Geographisches Institut der Universität Zürich: Zürich; 205.

Kääb A, Huggel C, Barbero S, Chiarle M, Cordola M, Epinfani F, Haeberli W, Mortasa G, Semino P, Tamburini A, Viazzo G. 2004. Glacier hazards at Belvedere glacier and the Monte Rosa east face, Italian Alps: Processes and mitigation. *Proceedings of the Interpraevent 2004*, Riva/Trient.

Kneisel C. 2003. Permafrost in recently deglaciated glacier forefields – measurements and observations in the eastern Swiss Alps and northern Sweden. *Zeitschrift für Geomorphologie N.F.* **47**(3): 289–305.

Krautblatter M, Dikau R. 2007. Towards a uniform concept for the comparison and extrapolation of rockwall retreat and rockfall supply. *Geografiska Annaler* **89A**(1): 21–40.

Krautblatter M, Moser M, Schrott L, Wolf J, Morche D. 2012. Significance of rockfall magnitude and carbonate dissolution for rock slope erosion and geomorphic work on Alpine limestone cliffs (Reintal, German Alps). *Geomorphology* **167–168**(15): 21–34.

Lipovsky PS, Evans SG, Clague JJ, Hopkinson C, Couture R, Bobrowsky P, Ekström G, Demuth MN, Delaney KB, Roberts NJ. 2008. The July 2007 rock and ice avalanches at Mount Steele, St. Elias Mountains, Yukon, Canada. *Landslides* **5**(4): 445–455.

Matsuoka N, Hirakawa K, Watanabe T, Haeberli W, Keller F. 1998. The role of diurnal, annual and millennial freeze–thaw cycles in controlling alpine slope instability. Proceedings of the Seventh International Conference on Permafrost, Yellowknife, Canada. *Collection Nordicana* **57**: 711–717.

Matsuoka N, Hirakawa K, Watanabe T, Moriwaki K. 1997. Monitoring of periglacial slope processes in the Swiss Alps: the first two years of frost shattering, heave and creep. *Permafrost and Periglacial Processes* **8**: 155–177.

Mazza A. 1998. Evolution and dynamics of Ghiacciaio Nord delle Locce (Valle Anzasca, Western Alps) from 1854 to the present. *Geografia Fisica e Dinamica Quaternaria* **21**: 233–243.

Mazza A. 2000. Some results of recent investigations on Ghiacciaio del Belvedere (Anzasca Valley, Western Alps) taking into account the glacier mechanism. *Geografia Fisica e Dinamica Quaternaria* **7**: 59–71.

Noetzli J, Hoelzle M, Haeberli W. 2003. Mountain permafrost and recent Alpine rock-fall events: a GIS-based approach to determine critical factors. *Proceedings of the 8th International Conference on Permafrost*, Zurich; 827–832.

Oppikofer T, Jaboyedoff M, Keusen H-R. 2008. Collapse at the eastern Eiger flank in the Swiss Alps. *Nature Geoscience* **1**: 531–535.

Post A, Lachapelle ER. 1971. *Glacier Ice*. University of Toronto Press: Toronto; 110

Pralong A, Funk M. 2006. On the instability of avalanching glaciers. *Journal of Glaciology* **52**(176): 31–48.

Rabatel A, Deline P, Jaillet S, Ravanel L. 2008. Rock falls in high-alpine rock walls quantified by terrestrial lidar measurements: a case study in the Mont Blanc area. *Geophysical Research Letters* **35**(10): L10502.

Ranzi R, Grossi G, Iacovelli L, Tscharner S. 2004. Use of multispectral ASTER images for mapping debris-covered glaciers within the GLIMS Project. *Proceedings of the IGARSS 2004*, Toulouse.

Rapp A. 1960. Recent development of mountain slopes in Kärkevagge and surroundings. *Northern Scandinavia. Geografiska Annaler* **42**: 65–201.

Ravanel L, Deline P. 2011. Climate influence on rockfalls in high-Alpine steep rockwalls: the north side of the Aiguilles de Chamonix (Mont Blanc massif) since the end of the Little Ice Age. *The Holocene* **21**: 357–365. DOI. 10.1177/0959683610374887

Röthlisberger H. 1981. Eislawinen und Ausbrüche von Gletscherseen. In *Gletscher und Klima – glaciers et climat, Jahrbuch der Schweizerischen Naturforschenden, Gesellschaft*, Kasser P (ed.). wissenschaftlicher Teil 1978. Birkhäuser Verlag: Berlin; 170–212.

Sass O. 2005. Spatial patterns of rockfall intensity in the northern Alps. *Zeitschrift für Geomorphologie N.F. Suppl*. **138**: 51–65.

Tamburini A, Mortara G. 2005. The case of the "Effimero" Lake at Monte Rosa (Italian Western Alps): studies, field surveys, monitoring. In *Proceedings of the 10th ERB Conference*, Turin, 13–17 October 2004, UNESCO, IHP-VI Technical Documents in Hydrology **77**: 179–184.

Wagner S. 1996. Dreidimensionale Modellierung zweier Gletscher und Deformationsanalyse von eisreichem Permafrost. In *Mitteilungen*. Laboratory of Hydraulics Hydrology and Glaciology: Zürich; vol. **146**.

Warburton J. 2007. Sediment budgets and rates of sediment transfer across cold environments in Europe: a commentary. *Geografiska Annaler* **89A**(1): 95–100.

Wegmann M, Gudmundsson GH, Haeberli W. 1998. Permafrost changes in rock walls and the retreat of Alpine glaciers: a thermal modelling approach. *Permafrost and Periglacial Processes* **9**: 23–33.

Zgraggen A. 2005. *Measuring and Modelling Rock Surface Temperatures in the Monte Rosa East Face*. Diploma Thesis: ETH Zurich.